Modeling of Arterial Spin Labeling Signals

David C. Alsop, Ph.D.
Beth Israel Deaconess Medical Center and
Harvard Medical School, Boston USA

Introduction

Arterial Spin Labeling (ASL)[1,2] is a remarkable and useful approach to the measurement of perfusion, sometimes referred to as regional blood flow. As will become apparent below, measurement of blood flow requires observations of the transport of a tracer. ASL is unique in that the tracer is the naturally occurring water in arterial blood, which is labeled by the application of magnetic fields. While the generation of an image that is fairly representative of perfusion requires relatively simple mathematics, more complex modeling and interpretation can assess limitations to the simplest model, provide more precise quantitative values, and potentially provide additional physiologic information.

The Simple Model

The ASL experiment involves the acquisition of multiple images with different labeling of arterial water. Most commonly, just two images, a labeled image and a control image, without labeling, are acquired and subtracted. Labeling is almost always performed by affecting the longitudinal magnetization. Mz. of the blood outside the imaged region. While novel forms of labeling include velocity selective labeling of blood already in the slice[3,4] or labeling of transverse magnetization by adiabatic half passage[5], the following discussion will be restricted to spatially selective labeling of Mz. The evolution of signal in a small region of tissue is given by the modified Bloch equation[1]

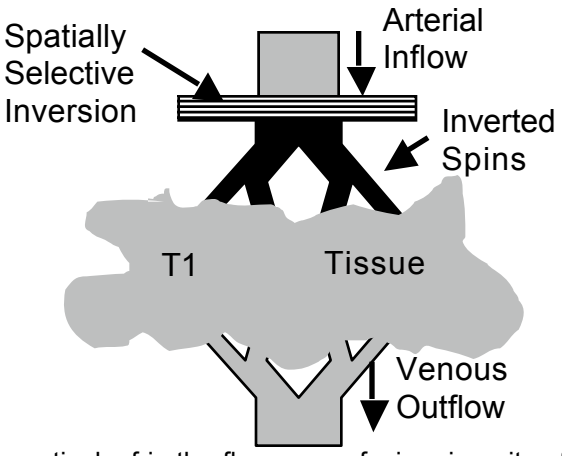

$$\frac{dM_t}{dt} = \frac{\left(M_t^0 - M_t(t)\right)}{T_{1t}} + f\rho_t\left(M_a(t) - M_v(t)\right)$$

where M refers to the longitudinal magnetization, the suffixes t, a and v are for tissue, arterial, and venous parameters respectively, f is the flow, or perfusion, in units of ml blood per s per gram of tissue, and ρ is the tissue density in g/ml. In this equation, the arterial and venous magnetization are those in the small vessels feeding the small region of tissue. Because of diffusion between the tissue and the capillaries and venules, the venous magnetization per water molecule is typically assumed equal to that in tissue. This freely diffusible tracer assumption is probably pretty good in most tissues, but is somewhat suspect in the brain, as only approximately 80% of water is extracted into the tissue in passage through the tight barriers of the cerebral microvasculature[6]. Defining the water content in one ml of blood or tissue as ρw_b and ρw_t, we can rewrite the Bloch equation as

$$\frac{dM_t}{dt} = \frac{\left(M_t^0 - M_t(t)\right)}{T_{1t}} + f\frac{M_t^0}{\lambda}\left(\frac{\rho w_t M_a(t)}{\rho w_b M_t^0} - \frac{M_t(t)}{M_t^0}\right) \qquad \lambda = \left(\frac{\rho w_t}{\rho_t \rho w_b}\right)$$

where we have defined the tissue-blood partition coefficient, λ, on the right. Consider the numerically simplest ASL study, the idealized steady state continuous labeling method[1]. In this approach, the arterial magnetization is maintained at a constant of either the equilibrium magnetization, M_a^0, for the control or $-M_a^0$ for the labeling. Over time a steady state is reached and the derivative goes to zero. Then the difference between the control and label magnetization is given by[1,7]

$$\frac{M_t^{cnt} - M_t^{lbl}}{M_t^{cnt}} = \frac{2}{\left(\frac{1}{T_{1t}} + \frac{f}{\lambda}\right)} \frac{f}{\lambda} \approx 2T_{1t} \frac{f}{\lambda} \qquad \text{where we have used } \frac{M_a^0}{M_t^0} = \frac{\rho w_b}{\rho w_t}$$

Since the image intensity is proportional to M, flow can be directly calculated from the images if T1 and λ are known, assumed, or measured. Another mathematically simple labeling scheme is where labeling of the form $-2M_a^0 \exp(-t/T_{1t}) + M_a^0$ is applied for time from 0 to TI corresponding to pulsed inversion of arterial blood for the label[8,9]. This gives a difference in magnetization at time TI of

$$\frac{M_t^{cnt} - M_t^{lbl}}{M_t^{cnt}} = -2\,TI \frac{f}{\lambda} \exp\left(-TI\left(\frac{1}{T_{1t}} + \frac{f}{\lambda}\right)\right) \left[\frac{\left(\exp\left(-TI\left(\frac{1}{T_{1b}} - \frac{1}{T_{1t}} - \frac{f}{\lambda}\right)\right) - 1\right)}{TI\left(\frac{1}{T_{1b}} - \frac{1}{T_{1t}} - \frac{f}{\lambda}\right)}\right] \approx 2\,TI \frac{f}{\lambda} \exp\left(-\frac{TI}{T_{1t}}\right)$$

where similar T1's of tissue and blood were assumed in the approximation on the right. Because ASL cannot be performed with labeling at the arteriole in most practical situations, additional complications arise.

Modeling of Arterial Transit

In practice, labeling is performed some distance away from the feeding arterioles because imperfections in RF pulses, magnetization transfer effects, and motion would introduce errors with close labeling. In many human tissues, the time required to move from the labeling region to the tissue is comparable to or longer than the T1 of blood. Failure to account for decay of the label during transit would give an erroneous measure of flow. The arteriolar labeling in the presence of a transit delay, δ, is related to the large vessel labeling by[7] $M_{arteriole}(t) = M_{artery}(t - \delta) \exp\left(-\frac{\delta}{T_{1b}}\right)$.

This expression shows that there are two uncertainties about the contribution of arterial blood labeled at a certain time. The first is whether the label actually reaches the arteriole before imaging and the second is how much the label has decayed in transit if it did reach the arteriole. If T1 is similar or the same in tissue and blood, then the second problem is minimal because the decay of the label depends only on time and not where the label is located. The first uncertainty, whether the label has reached the arteriole or not, can be eliminated by stopping all labeling and waiting sufficiently long, based on experience or expectation, that all of the label has entered the arterioles[7,10]. If one employs the transit correction above and a wait w, longer than δ, after labeling, then the idealized steady state ASL equations become[7]

$$\frac{M_t^{cnt} - M_t^{lbl}}{M_t^{cnt}} = \frac{2}{\left(\frac{1}{T_{1t}} + \frac{f}{\lambda}\right)} \frac{f}{\lambda} \exp\left(\delta\left(\frac{1}{T_{1t}} - \frac{1}{T_{1b}}\right)\right) \exp\left(-\frac{w}{T_{1t}}\right)$$

If w is longer than δ, then the dependence on δ is small unless there is a big difference between the blood and tissue T1. If w is too short, then there may be stronger dependence on δ as well as an additional complication, the presence of substantial labeled blood in larger arteries. Arteries longer than the voxel size will degrade spatial resolution if filled with labeled blood. These vessels must be suppressed by longer delay or flow dephasing gradients[1,11] to avoid quantification errors. However, vessels comparable in size to the voxel or smaller need not be a major problem.

Consider the case of a tissue with equal T1 to blood. Once the blood has entered an artery smaller than the voxel size, the signal observed is independent of whether the blood has passed through capillaries into tissue or not. One can make a two compartment model[7] with a vascular compartment

containing small arteries, arterioles and capillaries, and a tissue compartment. Assuming arrival of the label at the vascular compartment at a time δa and instantaneous exchange at the end of the capillary at a second time δt, one can calculate the signal as a function of flow by integration of the Bloch equations.

$$\frac{M_t^{cnt} - M_t^{lbl}}{M_t^{cnt}} = \frac{2}{\left(\frac{1}{T_{1t}} + \frac{f}{\lambda}\right)} \frac{f}{\lambda} \left[T_{1t} \exp\left(-\frac{\delta_t}{T_{1b}}\right) \exp\left(\frac{\min(\delta_t - w, 0)}{T_{1t}}\right) + T_{1b} \left(\exp\left(\frac{\min(\delta_a - w, 0) - \delta_a}{T_{1b}}\right) - \exp\left(\frac{\min(\delta_t - w, 0) - \delta_t}{T_{1b}}\right) \right) \right]$$

Measurements of the ASL difference signal for a range of different wait times can be fit to a model[12,13], as above, for the signal as a function of delay. For most tissues, the shape of the curve is not sufficient to differentiate δa and δt. Instead, fitting usually just provides a measure of δa. However, if flow dephasing gradients are employed to eliminate most vascular signal, a separate fit of δt can be performed. It has recently been suggested that the combination of δa, flow and δt measurement permits the calculation of the arterial blood volume[13].

A limitation to all of these modeling techniques is the assumption of a single constant delay time for all blood entering a voxel. Pulsatile flow over the cardiac cycle, multiple flow paths in borderzone areas, and simply laminar flow create a distribution of transit times. In the case of laminar flow without radial mixing, the distribution of transit times is given by[12]

$p(\delta) = \frac{2\delta_{\min}^2}{\delta^3}$ *for* $\delta > \delta_{\min}$ This model serves as an extreme for non plug flow. Fitting with this model produces significantly different transit times and curves shapes than for a constant transit delay.

The instantaneous and complete exchange of water with tissue in the capillaries has been questioned and modeled. One approach has been to assume a pool of well-mixed arterial blood in exchange with a tissue compartment[14]. An alternative approach is to model the entire capillary exchange process[15]. It is challenging to incorporate larger vessel delay effects and diffusive exchange processes in a single model.

Water density and relaxation effects

Previously we've assumed that the tissue-blood partition coefficient is known and that the signal is proportional to the magnetization density. In practice, the partition coefficient is not known and must be assumed[16]. The partition coefficient includes the tissue water density, something which those experienced with MR imaging know is not particularly uniform in tissue. If the sensitivity of the scanner is uniform, i.e. a uniform transmit and receive coil are used, one can use traditional methods for generating maps of relative water density[17]. Very long TR images or simultaneous T1 quantification can be used. Since tissue T1 is generally required in the quantification of flow, simultaneous T1 and proton density analysis is advantageous. To determine absolute water density, a region of fluid, such as CSF, can be used as a reference. However, one can show that the tissue water density in the partition coefficient cancels the water density contribution to Mt in flow quantification. Hence all that is really required is an estimate of the sensitivity to pure water at each voxel. In situations where sensitivity is nonuniform, as with array coils, a model for the sensitivity is required in order to accurately measure absolute blood flow. Techniques for coil sensitivity mapping have been rapidly advancing with the implementation of parallel imaging. In principle, the density of tissue is required to report flow in units of ml/gm/s or similar units. However, there is little intrinsic interest in the difference between flow in units of ml/gm/s and the related quantity in ml/ml/s.

An additional assumption of quantification is that the signal from the water depends only on the magnetization. Short T2 or T2* can cause attenuation of the signal which may not be mirrored in the coil sensitivity measurement[18]. When blood signal is not attenuated with dephasing gradients, different T2 and T2* in blood and tissue could cause deviations from the quantification theory. While transverse relaxation can be measured and modeled, using sequences with limited sensitivity to T2 and T2* is certainly preferable.

Measurement of T1 in tissue is frequently performed for ASL quantification, but T1 in blood is usually assumed based on literature measurements. Given the strong, exponential dependence of the ASL signal on blood T1, relatively small errors in blood T1 can cause large effects on the perfusion measurement. T1 of blood is sensitive to the hematocrit[19], as is perfusion itself[20], so in-vivo measurement of T1 may become necessary. Even with an in-vivo measurement, complications remain because of the lower microvascular hematocrit, and the potential for regional variations in hematocrit[21].

Time Series Analysis

While not always the case, ASL is typically performed with single-shot imaging, such as echoplanar, that acquires images in a few seconds. Attaining sufficient SNR, however, requires repeated scanning and typically the label and control images are interleaved in time. In many applications, motion or other nonthermal noise is a major source of variance in the image time series. While these noise sources can be substantially reduced by acquisition with background suppression[22,23,24], post-processing techniques such as motion correction, principal component analysis[25] and independent component analysis[26] that are in wide use for BOLD fMRI can also find application in ASL. When ASL itself is used for activation studies, the techniques of BOLD are complicated by the introduction of control images at various times during the sequence[27].

Applications of ASL MRI

ASL is advantageous in several ways: it uses no external contrast, it permits a reproducible and reasonably accurate measure of absolute blood flow, it is not inherently sensitive to large vessels, and with the appropriate sequence, it is insensitive to susceptibility induced magnetic field variations. For all of these reasons, it has found application in brain activation studies, animal investigations, and clinical studies of cerebral and body abnormalities. These applications are reviewed in a separate syllabus contribution by this author, for the Advanced Brain MR Imaging course.

References

1. Williams, D.S. et al., *Proc. Natl. Acad. Sci. USA* 89; 212-216 (1992).
2. Detre, J.A. et al. *Magn Reson Med*. 23:37-45 (1992)
3. Wong, E.C. et al. *Proc 9'th ISMRM* p. 621 (2002)
4. Duhamel, G et al. *Magn Reson Med*. 50:145-153 (2003)
5. Marro, K. *J Magn Reson*. 124:240-244 (1997)
6. Raichle, M.E. et al. *Am. J. Physiol*. 230:543-552 (1976)
7. Alsop, D.C. et al., *J. Cereb. Blood Flow Metab.* 16; 1236-1249 (1996).
8. Edelman RR et al., *Radiology* 192:513-520 (1994
9. Kwong, K.K. et al., *Magn Reson Med* 34:878-887 (1995)
10. Wong E.C. et al., *Magn Reson Med* 39:702-708 (1998)
11. Ye, F.Q. *Magn Reson Med* 37:226-235 (1997)
12. Gonzalez-At, J.B. et al. *Magn Reson Med*. 43:739-746 (2000)
13. Wang, J. et al. *Magn Reson Med*. 50:599-607 (2003)
14. Parkes, L.M. et al. *Magn Reson Med*. 48:27-41 (2002)
15. Ewing, J.R. *Magn Reson Med*. 46:465-475 (2001)
16. Herscovitch, P. et al. *J Cereb Blood Flow Metab*. 5:65-69 (1985)
17. Roberts, D.A. et al. *J. Magn Reson Imaging*. 6:363-366 (1996)
18. St. Lawrence, K.S. et al. *Magn Reson Med.* 53:425-433 (2005)
19. Lu, H. et al. *Magn Reson Med*. 52:679-682 (2004)
20. Floyd, T.F. et al. Ann Thorac Surg. 76:2037-2042 (2003)
21. Yamauchi, H. et al. *Stroke*. 29:98-103 (1998)
22. Dixon, W.T. et al. *Magn Reson Med*. 18:257-268 (1991)
23. Ye, F.Q. et al., *Magn Reson Med* 44:92-100 (2000
24. Garcia, D.M. et al. *Magn Reson Med*. 53:366-372 (2005)
25. Alsop, D.C. et al. *Proc. 5'th ISMRM* p. 1687 (1997)
26. Perthen, J.E. et al. *Proc. 12'th ISMRM* p.1359 (2004)
27. Aguirre, G.K. et al. *Neuroimage* 15:488-500 (2002)